Centrifuge modelling of cyclic multidirectional loading of suction anchors in clay for floating wind arrays

C.G. O'Donovan, M. Long
University College Dublin, Ireland, christopher.odonovan2@ucdconnect.ie, mike.long@ucd.ie

C. Lyu, L. Arentz-Hansen
Oslo Metropolitan University, Norway, chuangxin.lyu@oslomet.no, ludvig.arentz-hansen@sweco.no

E. Sorlie, I.R. Jahren, I. Liplass
Multiconsult, Oslo, Norway, erik.sorlie@multiconsult.no, ingerid.jahren@multiconsult.no, ingrid.liplass@multiconsult.no

L.A. Jones, R. Herzog., A. Marin, I. Anastasopoulos
ETH, Zürich, Switzerland, liam.jones@igt.baug.ethz.ch, ralf.herzog@igt.baug.ethz.ch, alexandru.marin@igt.baug.ethz.ch, ioannis.anastasopoulos@igt.baug.ethz.ch

ABSTRACT: Given the wind energy potential in deeper coastal waters, offshore wind development is expected to expand from primarily fixed-bottom foundation technology to include floating wind turbine platforms. While floating wind is technically feasible, its cost remains prohibitively high, with mooring and anchorage systems constituting a significant proportion of the overall expense. Sharing anchors among multiple floating platforms in an array can reduce these costs, but it also introduces complex multidirectional loading, under which the performance of many anchors remains uncertain. This study investigates the capacity of shared suction caisson anchors using centrifuge modelling of a wished-in-place anchor in normally to over-consolidated kaolin clay. Monotonic and cyclic load cases were investigated using a single-mooring configuration to understand baseline performance, where the average and cyclic load directions are collinear. Multidirectional loading was then assessed using a dual-mooring configuration to evaluate the effects of misalignment between the average and cyclic load directions. The results reveal similar cyclic hardening under both multidirectional and collinear conditions for the investigated system under the applied loads. This study provides experimental insights into the behaviour of suction anchors in clay subjected to multidirectional cyclic loading and should facilitate future research on the subject.

1 INTRODUCTION

As the development of offshore wind energy infrastructure progresses to meet renewable energy goals, a shift into deeper waters (> 60 m) appears necessary (IEA, 2023), where floating offshore wind turbines (FOWTs) become a viable technology (Bachynski, 2018; Goupee et al., 2014). Such an expansion of offshore infrastructure presents a vast technical and logistical challenge (Gourvenec, 2024; Gourvenec et al., 2022), highlighting the need for refined and optimised technologies. Sharing anchors between platforms in an array of FOWTs has the potential to reduce both material costs and offshore survey burden (Devin et al., 2021; Fontana et al., 2018; Xu et al., 2024). To this end, suction anchors present an efficient technology (Cerfontaine et al., 2023) which has been demonstrated as a feasible solution to moor FOWTs in a shared configuration (Frossard et al., 2025). Experimental work is required to establish a robust understanding of cyclic multidirectional loading (Soriano et al., 2025).

Experimental and numerical studies suggest that traditional unidirectional models for piles in sand may underestimate lateral displacements and the resultant forces in shared anchors for FOWTs (Chalhoub et al., 2025; Jenck et al., 2021; Rudolph et al., 2014). Furthermore, multidirectional element tests on sand (Sun and Biscontin, 2025; Wen et al., 2025) and clay (Bi et al., 2025) suggest that the complex stress histories generated by multidirectional loading are generally detrimental to soil strength. The cyclic behaviour of clays is generally well-characterised under conventional loading, with the accumulation of pore pressure dictating failure in undrained conditions (Andersen, 2015). Furthermore, post-cyclic consolidation arises as a result of the dissipation of these pore pressures, leading to potentially large strength gains (O'Loughlin et al., 2020), of particular interest when considering entire life design (Laham et al., 2025). How multidirectional loading may alter the response of soils around a structure and dissipation of excess pore pressure is an area of ongoing research (Abadie, 2025; Soriano et al., 2026).

This project contributes to the body of knowledge on suction anchors for shared mooring of floating offshore wind turbines (FOWTs). A series of centrifuge tests on suction caisson models installed in a normally to over-consolidated kaolin clay were conducted at the ETH-Zürich Geotechnical Centrifuge Centre (GCC), using the 8.25 m diameter 500 gton beam centrifuge. The primary objective of this work is to generate experimental data on shared anchors for floating offshore wind development. Future post-test numerical analysis will further assess constitutive model and finite element model accuracy.

2 PHYSICAL MODEL TESTS

Dry kaolin powder, described in Table 1, was reconstituted as a slurry, mixed under vacuum at a moisture content of greater than twice the liquid limit. The material was then incrementally loaded to a vertical stress of 150 kPa at 1g in 400 mm diameter strongboxes, shown in Figure 1.

Table 1. K1 Kaolin properties.

Property	**Value**
Specific Gravity (g/cm^3)	2.675*
Liquid Limit (LL) (%)	50
Plastic Limit (PL) (%)	35
s_u/σ'_0 (-)	0.265 (triaxial)*
c_v (mm^2/s)	0.1-0.3

*(Antoniou et al., 2024)

A 100 mm tall (L), 50 mm diameter (D) model caisson, with a wall thickness of 2 mm was installed at 1g, by jacking into the kaolin, after which mooring line(s) were connected to padeyes located on the lid of the model, at 35° inclination. The system was then spun to 100g and the kaolin allowed achieve final consolidation in flight.

Loading could be applied to the caisson by two actuators, a primary hydraulically powered dynamic actuator controlled via a highspeed proportional-integral-derivative (PID) loop with cyclic capability and a secondary electrically powered actuator, controlled via a simple static PID loop, as annotated in Figure 2. Loads were corroborated at the terminus of the mooring cables using in-line load cells close to the anchor padeyes Displacements were monitored using a combination of laser sensors, shown in Figure 1, and discrete image correlation (DIC) using photographs captured from two fixed lens, global shutter cameras, shown in Figure 2.

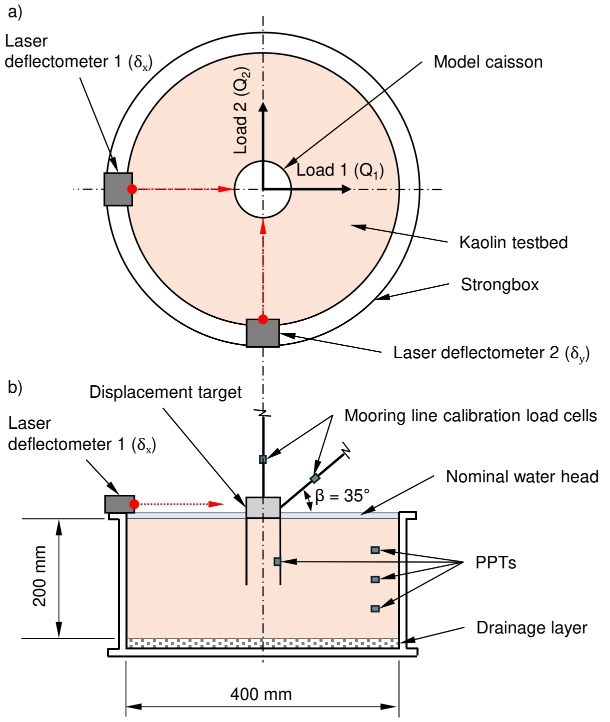

Figure 1. Experimental design, indicating instrumentation and strong-box arrangement.

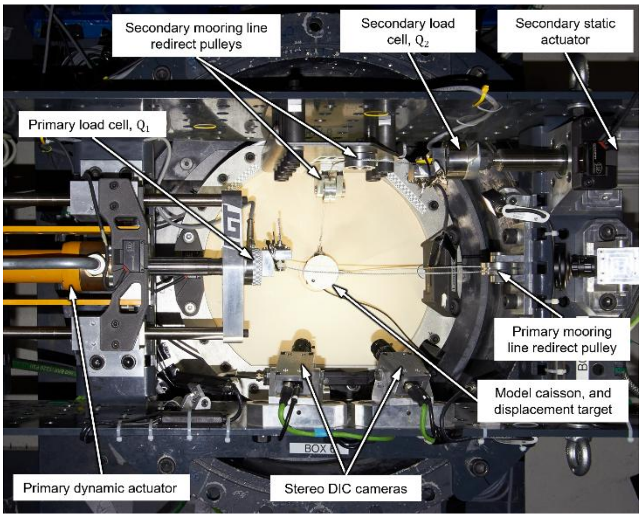

Figure 2. Annotated photograph illustrating the achieved arrangement of load actuators and cells, mooring cables and redirect system and DIC camera instrumentation.

The test programme consisted of three load cases designed to establish a baseline and then simulate increasing cyclic loading as an analogue for storm loading (Zografou et al., 2018). The parameters of the three load cases investigated are detailed in Table 2.

Displacements and rotations shown in Figure 3 were calculated using DIC analysis and directly from the two horizontally orientated laser deflection sensors.

Table 2. Load cases

Load Case	Loding rate/ frequency	$\frac{Q_{cyclic}}{Q_{ave}}$	$\frac{Q_{y\,ave}}{Q_{x\,ave}}$	ω (°)
Monotonic	2 mm/s	-	0.0	-
Unidirectional cyclic	5 Hz	0.6	0.0	0
Multidirectional cyclic	5 Hz	0.6	1.0	28 - 81

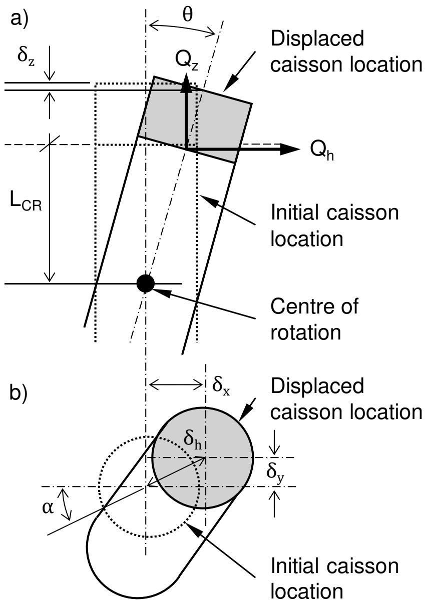

Figure 3. a) side elevation rotation and displacements and b) plan horizontal displacements.

The initial test was a constant rate of displacement monotonic pull test, in a single (unidirectional) mooring configuration, via the primary actuator (Q_1) which is aligned to the x-z plane. This test was conducted at a rate of displacement of 2 mm / s, chosen to create primarily undrained conditions in the kaolin around the model, using dimensionless velocity, V > 30 (Randolph, 2004). The loads from this initial test provided the target for the following cyclic load cases.

$$V = \frac{vD}{c_v} \tag{1}$$

The second load case is a cyclic loading case applied via a single (unidirectional) mooring line connected to the primary actuator (Q_1), and so all loads are also in the x-z plane. The load packages for this case were selected to maintain a constant ratio between the cyclic (Q_{cyclic}) and average (Q_{ave}) load components, while the magnitude of the load was increased by a constant increment over the series of packages. A loading frequency of 5 Hz was selected to create primarily undrained loading conditions by substituting v for the product of load frequency and the caisson diameter, D in equation 1.

The third and final load case aimed to replicate the second load case but applied via two mooring lines to create a multidirectional load with other conditions equal. To achieve this, the multidirectional load case was applied such that the magnitudes of the cyclic and average load components were equal to that of the unidirectional load case but applied via two mooring lines. Thus, in the third load case, the average load was applied via both the secondary (Q_2) and primary (Q_1) mooring lines and actuators, while the cyclic component was applied only via the primary mooring line (Q_1), per Figure 4. As Q_1 is aligned to the x-z plane and Q_2 the y-z plane, the horizontal components of the loads are orthogonal and the x and y components of the resultant load can be calculated using the cosine of the mooring angle, which was the same for both the primary and secondary mooring lines.

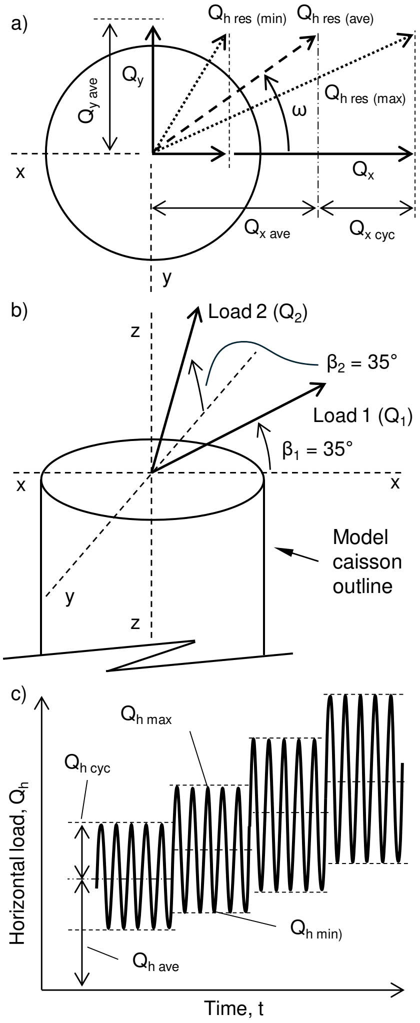

Figure 4. (a) horizontal and (b) isometric load arrangements and (c) schematic time series loading sequence.

Parity was sought between the average and cyclic components of the horizontal loads in the unidirectional and multidirectional load cases. However, a cyclic load could only be applied in x direction, via load Q_1, while an average load could be applied in both the x and y directions, via a combination of loads Q_1 and Q_2, illustrated in Figure 4. The cyclic loads where therefore equal in the unidirectional and multidirectional cases, while, average loads were applied via either one or a combination of both mooring lines in the unidirectional and multidirectional cases, respectively. Under inclined multidirectional loading, the resultant vertical load is the algebraic sum of the vertical components in each mooring line, the effects of which are documented for shared anchors (Dias et al., 2025). In this experiment, as the horizontal average loads are the same between unidirectional and multidirectional cases, the average component of the vertical load (Q_z) which is shown in Figure 3, will be approximately 40% larger in the multidirectional case compared to the unidirectional case, per equation 2 that follows.

$$Q_{z\,ave,\;multi} = \sqrt{2} \cdot Q_{z\,ave,\;uni} \qquad (2)$$

As cyclic loads were applied only via the primary mooring line, the vertical component of cyclic loads are equivalent between cases.

$$Q_{z\,cyc,\;multi} = Q_{z\,cyc,\;uni} \qquad (3)$$

The implications of the larger average vertical load under multidirectional loading should be nominal as the weight of the caisson structure at 100g (~432 N) far exceeded any imposed upward average vertical load. However, it will be important to keep this in mind when assessing failure mechanisms.

3 RESULTS AND DISCUSSION

3.1 Monotonic loading

Monotonic loading under a constant rate of displacement was performed to establish the baseline response of the system. Rotations captured by the DIC system, until 12°, indicate a linear correlation between horizontal displacement suggesting a rotational mode of failure with a centre of rotation, L_{CR}, of 0.85*L*, which is defined in Figure 3. The monotonic capacity of the model caisson is 0.2 kN, employing a lateral displacement failure criterion of 0.1D, as proposed by Leblanc, Houlsby & Byrne, (2009), which guided the cyclic load targets to follow. The caisson was, however, able to hold a much higher ultimate load, should larger lateral displacements be tolerable.

Vertical and horizontal displacements in the x, y and z directions indicate primary displacement along the load direction, x, with some nominal displacement in the y direction. The caisson initially displaces vertically downward and then upward in the z direction. A small porewater pressure response is seen until about 10 mm horizontal displacement, which initially begins to dissipate before increasing again at larger lateral displacements around 30 mm.

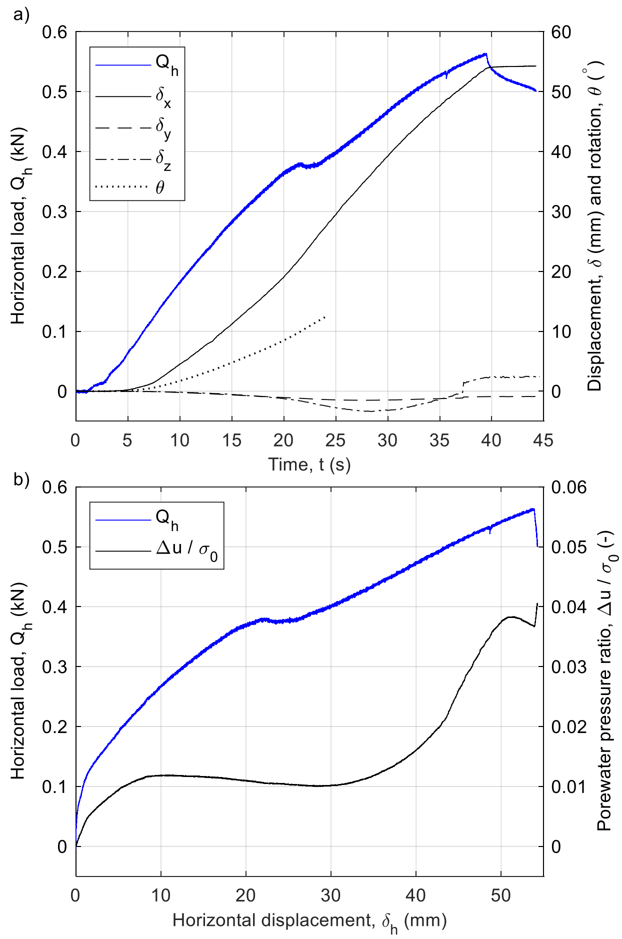

Figure 5. a) Monotonic horizontal load and displacement results in the time domain, and b) load and porewater pressure response in the horizontal displacement domain.

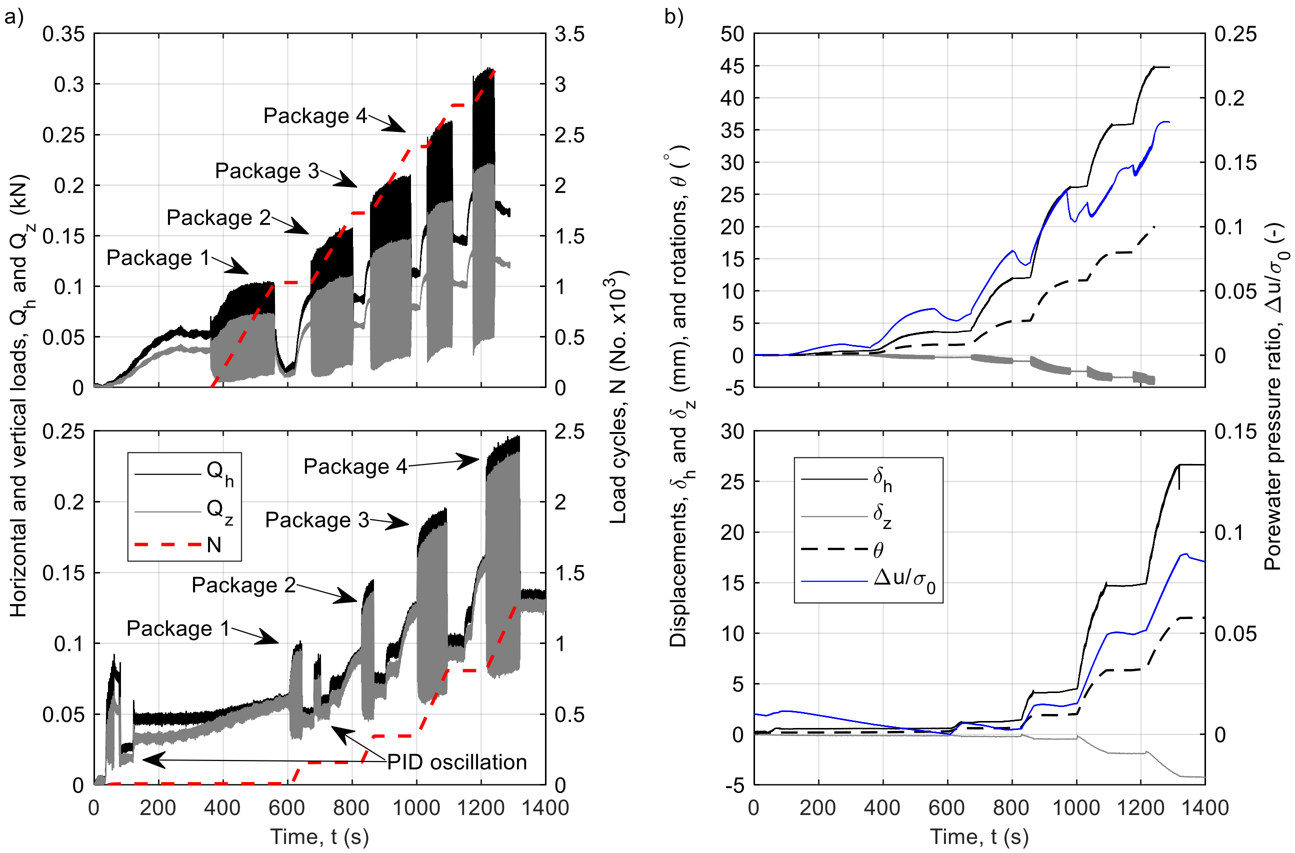

Figure 6. Results of unidirectional (top) and multidirectional (bottom) loading tests: (a) horizontal and vertical load as a function of time; and (b) accumulated displacements, rotation and normalised porewater pressures.

3.2 Cyclic loading

Cyclic loading was investigated in two tests, the time domain results of which are provided in Figure 6. Horizontal and vertical unidirectional loads, Q_h and Q_z, are shown against time in Figure 6 a (top left). Figure 6 b (top right) provides the lateral displacements and accumulated pore water pressure response for the model under these loads. Figure 6 a) and b) (bottom) provide comparative data from multidirectional loading. Load cycle count, N, is plotted against time in Figure 6 a) for each load case (top and bottom) and is based on measurement of peaks in the load versus time signal. The behaviour of the caisson in the load cases in Figure 6 exhibits a slight hardening response with increasing cycles, which is explored in further detail in the figures that follow. Based on the accumulating pore pressures, however, a softening response would be expected. Thus, it is possible that the observed response is due to rotation and alignment of the caisson with the load direction. This may also be an inherent material behaviour with significant softening only occurring when stresses in the failure zone approach critical state. Both unidirectional and multidirectional data suggest rotational failure modes with a similar centre of rotation, L_{CR}, (defined in Figure 3) compared to monotonic loading of where the centre of rotation was measured as 0.9L.

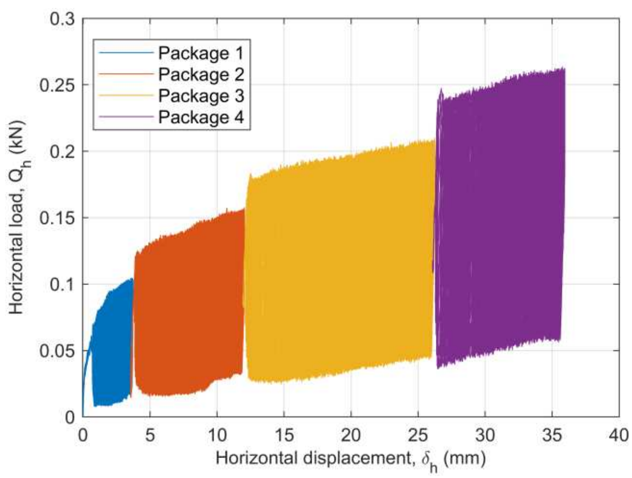

Figure 7. Unidirectional horizontal load versus horizontal displacements.

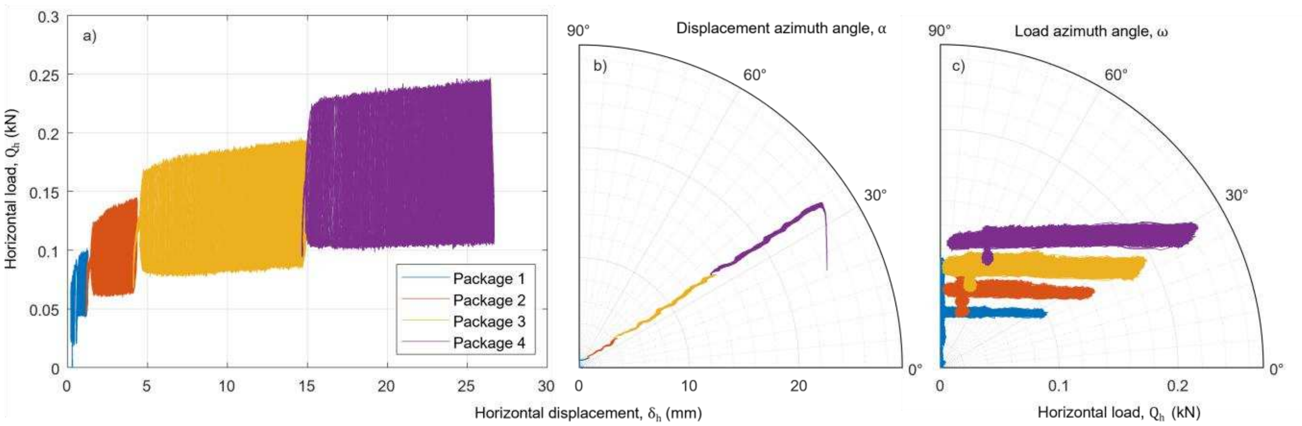

Figure 8. (a) multidirectional horizontal load versus horizontal displacements, (b) and (c) polar coordinate plots of displacement and load against respective azimuth angles α and ω.

Horizontal load is shown against displacement for the unidirectional cyclic load case (Figure 7). Each load package is a unique colour, maintained throughout the figures that follow to allow comparison between load cases and packages.

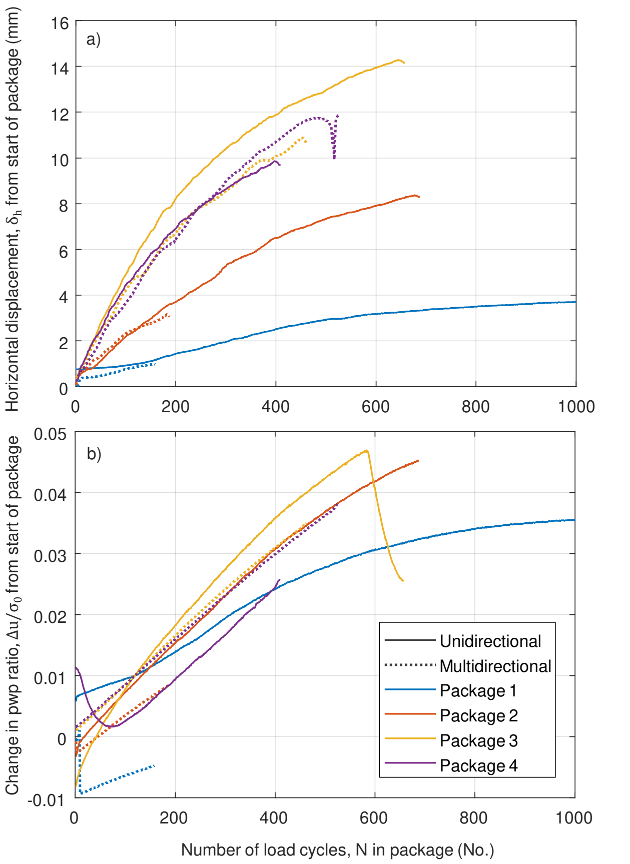

Figure 9. a) accumulated displacements per load package, and, b) accumulated porewater pressure per load package, for both unidirectional and multidirectional load cases.

Similarly, the resultant horizontal load and displacement for the multidirectional load case are shown in Figure 8 a). Polar coordinate plots of displacement and load against the respective displacement and load vector azimuth angles and also provided in Figure 8 b) and c), that illustrate the spread of the direction of displacements and loads achieved during the experiment.

Comparison of displacements and porewater pressure accumulations against load cycle count in Figure 9 indicates that multidirectional loading did not appear to have a notable impact on anchor response compared to the unidirectional case. This comes with the caveat of not being able to compare exact cyclic load histories (see Figure 6), but still illustrates that a similar overall cyclic response may occur under these two distinct load conditions.

4 CONCLUSION

Multidirectional loading arises when anchors are shared between turbines of an offshore wind array, a strategy that can be employed to improve the economics of floating wind energy infrastructure. This centrifuge test campaign set out to investigate the behaviour of suction anchors in a normally to over-consolidated clay under multidirectional cyclic loading to provide insight regarding shared anchors. Initially, monotonic loading of the 1:100 scale model caisson was conducted to establish its baseline strength. Secondly, cyclic loading behaviour of the model was established under unidirectional cyclic loading conditions, which maintained an approximate ratio of 0.6 between cyclic and average load magnitudes. Finally, comparative cyclic loading was conducted under multidirectional cyclic conditions.

The data presented here indicates that, under the cyclic loading investigated, displacement and porewater pressure response was similar under both unidirectional and multidirectional loading. This is highly relevant and a promising finding of interest to offshore wind developments in deeper waters, where the costs are still prohibitively high. Further work is required to illustrate repeatability and to generalise the findings of this experiment. Another interesting finding is the apparent hardening under both the unidirectional and multidirectional load conditions investigated, even as larger cyclic loads were applied. This is relevant to floating wind anchor design because the displacement and station keeping requirements are not necessarily the same as those of fixed-bottom wind turbines or floating offshore oil and gas platforms for which design philosophies are optimised.

ACKNOWLEDGEMENTS

The authors would like to acknowledge the technical team at ETH-Zürich GCC, as well as the EU Geolab scheme which funded this project under the European Union's Horizon 2020 Research and Innovation Programme (grant agreement No. 101006512).

REFERNECES

Abadie, C.N., 2025. Shared Anchor Pile Response to Multi-Directional Lateral Cyclic Loading, in: Proceedings of the 5th International Symposium on Frontiers in Offshore Geotechnics. Nantes, France.

Andersen, K., 2015. Cyclic soil parameters for offshore foundation design. The 3rd McClelland Lecture., in: The Third ISSMGE McClelland Lecture at Frontiers in Offshore Geotechnics III.

Antoniou, M., Gelagoti, F., Herzog, R., Kourkoulis, R., Anastasopoulos, I., 2024. Offshore foundations in low-plasticity cohesive soils: Cyclic degradation experimental evidence and simplified numerical analysis. Ocean Engineering 292, 116495. https://doi.org/10.1016/j.oceaneng.2023.116495

Bachynski, E.E., 2018. Fixed and Floating Offshore Wind Turbine Support Structures, in: Offshore Wind Energy Technology. John Wiley & Sons, Ltd, pp. 103–142. https://doi.org/10.1002/9781119097808.ch4

Bi, Q., Zhang, Y., Suzuki, Y., Lyu, C., 2025. Experimental study of soils under cyclic loading with direction varying about a mean direction, in: Proceedings of the 5th International Symposium on Frontiers in Offshore Geotechnics. Nantes, France.

Cerfontaine, B., White, D., Kwa, K., Gourvenec, S., Knappett, J., Brown, M., 2023. Anchor geotechnics for floating offshore wind: Current technologies and future innovations. Ocean Engineering 279, 114327. https://doi.org/10.1016/j.oceaneng.2023.114327

Chalhoub, R., Jenck, O., Kochnev, A., Liaudat, J., Dano, C., Abadie, C.N., Szymkiewicz, F., Katabi, M.K.A., Zachert, H., 2025. Floating wind turbine anchor piles under lateral multidirectional cyclic loading: experimental investigation, in: Proceedings of the 5th International Symposium on Frontiers in Offshore Geotechnics. Nantes, France.

Devin, M.C., DuPont, B.L., Hallowell, S.T., Arwade, S.R., 2021. Optimizing the Cost and Reliability of Shared Anchors in an Array of Floating Offshore Wind Turbines. ASME J. Risk Uncertainty Part B 7. https://doi.org/10.1115/1.4051163

Dias, X., Cerfontaine, B., Wen, K., 2025. Finite element analysis of a shared pile anchor in sand under inclined multidirectional cyclic loading, in: Proceedings of the 5th International Symposium on Frontiers in Offshore Geotechnics. Presented at the ISFOG5, Nantes, France.

Fontana, C.M., Hallowell, S.T., Arwade, S.R., DeGroot, D.J., Landon, M.E., Aubeny, C.P., Diaz, B., Myers, A.T., Ozmutlu, S., 2018. Multiline anchor force dynamics in floating offshore wind turbines. Wind Energy 21, 1177–1190. https://doi.org/10.1002/we.2222

Frossard, R., Bendzovski, R., Tuveng, E., 2025. Hywind Tampen – A geotechnical- and structural design of shared suction anchors, from concept to installation, in: Proceedings of the 5th International Symposium on Frontiers in Offshore Geotechnics. Nantes, France.

Goupee, A.J., Koo, B.J., Kimball, R.W., Lambrakos, K.F., Dagher, H.J., 2014. Experimental Comparison of Three Floating Wind Turbine Concepts. J. Offshore Mech. Arct. Eng 136. https://doi.org/10.1115/1.4025804

Gourvenec, S., 2024. Offshore geotechnical challenges of the energy transition. Geomechanics for Energy and the Environment 39, 100584. https://doi.org/10.1016/j.gete.2024.100584

Gourvenec, S., Sturt, F., Reid, E., Trigos, F., 2022. Global assessment of historical, current and forecast ocean energy infrastructure: Implications for marine space planning, sustainable design and end-of-engineered-life management. Renewable and Sustainable Energy Reviews 154, 111794. https://doi.org/10.1016/j.rser.2021.111794

IEA, 2023. Net Zero Roadmap: A Global Pathway to Keep the 1.5 °C Goal in Reach (No. (2023), Net Zero Roadmap: A Global Pathway to Keep the 1.5 °C Goal in Reach, IEA, Paris , Licence: CC BY 4.0). IEA, Paris.

Jenck, O., Obaei, A., Emeriault, F., Dano, C., 2021. Effect of Horizontal Multidirectional Cyclic Loading on Piles in Sand: A Numerical Analysis. Journal of Marine Science and Engineering 9, 235. https://doi.org/10.3390/jmse9020235

Laham, N., Kwa, K., Suzuki, Y., White, D., Gourvenec, S., 2025. Effect of episodic pre-failure cyclic loading on whole-life geotechnical properties of soft clays. Geotechnique 1–12. https://doi.org/10.1680/jgeot.24.00063

Leblanc, C., Houlsby, G.T., Byrne, B.W., 2009. Response of stiff piles in sand to long-term cyclic lateral loading. Geotechnique 60, 79–90. https://doi.org/10.1680/geot.7.00196

O'Loughlin, C., Zhou, Z., Stanier, S., White, D., 2020. Load-controlled cyclic T-bar tests: a new method to assess effects of cyclic loading and consolidation.

Geotechnique Letters 10, 7–15. https://doi.org/10.1680/jgele.19.00030
Randolph, M., 2004. Characterisation of soft sediments for offshore applications, in: Da Fonseca, A.V., Mayne, P.W. (Eds.), Proceedings of the 2nd International Conference on Site Characterization. Millpress Science, pp. 209–232.
Rudolph, C., Bienen, B., Grabe, J., 2014. Effect of variation of the loading direction on the displacement accumulation of large-diameter piles under cyclic lateral loading in sand. Can. Geotech. J. 51, 1196–1206. https://doi.org/10.1139/cgj-2013-0438
Soriano, C., Blanc, M., Cerfontaine, B., Thorel, L., 2026. Centrifuge modelling of suction anchors under multidirectional loading for shared mooring applications. International Journal of Physical Modelling in Geotechnics 1–17. https://doi.org/10.1680/jphmg.25.00031
Soriano, C., Thorel, L., Blanc, M., Audrain, P., 2025. Centrifuge modelling of cyclic loading on suction anchors in soft clay, in: Proceedings of the 5th International Symposium on Frontiers in Offshore Geotechnics. Presented at the 5th International Symposium on Frontiers in Offshore Geotechnics.
Sun, M., Biscontin, G., 2025. Conical Failure Surface of Medium-Dense Hostun Sand in Undrained Multidirectional Simple Shear Tests. J. Geotech. Geoenviron. Eng. 151, 04024156. https://doi.org/10.1061/JGGEFK.GTENG-10565
Wen, K.Z., Buckley, R.M., Byrne, B.W., 2025. Multidirectional perpendicular drained cyclic behaviour of a marine sand, in: Proceedings of the 5th International Symposium on Frontiers in Offshore Geotechnics. Nantes, France.
Xu, H., Rui, S., Shen, K., Jiang, L., Zhang, H., Teng, L., 2024. Shared mooring systems for offshore floating wind farms: A review. Energy Reviews 3, 100063. https://doi.org/10.1016/j.enrev.2023.100063
Zografou, D., Gourvenec, S., O'Loughlin, C.D., 2018. Response of normally consolidated kaolin clay under irregular cyclic loading and comparison with predictions from the accumulation procedure. Geotechnique 69, 106–121. https://doi.org/10.1680/jgeot.16.P.340